Published in final edited form as:

Oncogene. 2009 January 15; 28(2): 257–269. doi:10.1038/onc.2008.381.

MITOSTATIN, a Putative Tumor Suppressor on Chromosome 12q24.1, is Down-regulated in Human Bladder and Breast Cancer

A Vecchione[1,5,7], **M Fassan**[1,6,7], **V Anesti**[2], **A Morrione**[1], **S Goldoni**[3], **G Baldassarre**[4], **D Byrne**[1], **D D'Arca**[1], **JP Palazzo**[3], **J Lloyd**[3], **L Scorrano**[2], **LG Gomella**[1], **RV Iozzo**[3], and **R Baffa**[1]

[1]Department of Urology, Kimmel Cancer Center, Thomas Jefferson University, Philadelphia, Pennsylvania, USA

[2]Dulbecco-Telethon Institute, Venetian Institute of Molecular Medicine, Padova, Italy

[3]Department of Pathology, Anatomy and Cell Biology, Kimmel Cancer Center, Thomas Jefferson University, Philadelphia, Pennsylvania, USA

[4]Division of Experimental Oncology 2, CRO-IRCCS, Aviano, Italy.

Abstract

Allelic deletions on human chromosome 12q24 are frequently reported in a variety of malignant neoplasms, indicating the presence of a tumor suppressor gene(s) in this chromosomal region. However, no reasonable candidate has been identified so far. In this study, we report the cloning and functional characterization of a novel mitochondrial protein with tumor suppressor activity, henceforth designated *MITOSTATIN*. Human *MITOSTATIN* was found within a 3.2-kb transcript which encoded a ~62 kDa, ubiquitously-expressed protein with little homology to any known protein. We found homozygous deletions and mutations of *MITOSTATIN* gene in ~5% and ~11% of various cancer-derived cells and solid tumors, respectively. When transiently over-expressed, MITOSTATIN inhibited colony formation, tumor cell growth and was pro-apoptotic, all features shared by established tumor suppressor genes. We discovered a specific link between MITOSTATIN over-expression and down-regulation of Hsp27. Conversely MITOSTATIN knock-down cells showed an increase in cell growth and cell survival rates. Finally, MITOSTATIN expression was significantly reduced in primary bladder and breast tumors, and its reduction was associated with advanced tumor stages. Our findings support the hypothesis that MITOSTATIN has many hallmarks of a classical tumor suppressor in solid tumors and may play an important role in cancer development and progression.

Correspondence: Dr. Raffaele Baffa, Department of Urology, Thomas Jefferson University, 233 South 10th Street, BLSB 526, Philadelphia, PA 19107. Phone: 215-955-9072; Fax: 215-503-2627; E-mail: R_Baffa@mail.jci.tju.edu.

[5]Dr. Vecchione's current address is Division of Pathology, II Faculty of Medicine, University "La Sapienza," Ospedale Sant' Andrea, Rome, Italy.

[6]Dr. Fassan's current address is Department of Diagnostic Medical Sciences and Special Therapies, Pathology Unit, University of Padova, Padova, Italy.

[7]These authors contributed equally to this work.

Keywords

Bladder cancer; breast cancer; mitochondria; chromosome 12q; tumor suppressor

Introduction

During the course of cancer development, a normal cell progresses towards malignancy by acquiring a specific series of mutations (Hanahan and Weinberg, 2000). Over the past decades, genetic studies have demonstrated that cancer cells accumulate DNA changes that activate oncogenes and inactivate tumor suppressor genes. The role of tumor suppressor genes in neoplastic development is crucial, given that reintroduction of one or more of these genes into cells in which their function is compromised can completely revert the neoplastic phenotype. Therefore, it is not surprising that several tumors show a high frequency of loss of heterozygosity (LOH) at specific chromosomal regions encompassing tumor suppressor genes. Loss of heterozygosity in the telomeric regions of chromosome 12 has been observed in many solid tumors, such as breast (Aubele *et al.*, 2000; Tirkkonen *et al.*, 1997), lung (Shiseki *et al.*, 1996), gastric, and prostate cancers (Sattler *et al.*, 1999; Schmutte *et al.*, 1997), pancreatic adenocarcinoma (Kimura *et al.*, 1998), head and neck squamous cell carcinoma (Field *et al.*, 1995), distal bile duct carcinoma (Rijken *et al.*, 1999), renal cell carcinomas (Jiang *et al.*, 1998), and urothelial carcinoma of the urinary bladder (Koo *et al.*, 1999). These observations support the concept that cloning and characterization of tumor suppressor genes may lead to the development of novel therapies for malignant tumors.

In the process of screening for genes expressed during growth arrest induced by the small leucine-rich proteoglycan decorin (Csordas *et al.*, 2000; Goldoni *et al.*, 2007; Moscatello *et al.*, 1998; Santra *et al.*, 1997; Santra *et al.*, 1995; Xu *et al.*, 2002), we identified an EST that was up-regulated in three different growth-suppressed tumor cell lines (i.e.: decorin-transfected tumor cells). We investigated in more detail the nature of one of these ESTs for several reasons. First, its key chromosomal location is a known fragile site in cancer. Second, the overexpression of this gene product was induced by decorin, a growth-inhibitory protein (Goldoni *et al.*, 2007; Santra *et al.*, 1997). Third, it is well established that the regulatory effect on cell growth may be mediated by variations on the level of expression of downstream genes via a paracrine or autocrine mechanism.

In this study, we described the cloning of a novel putative tumor suppressor gene (previously identified as Ts12q for tumor suppressor at 12q) and named it MITOSTATIN, for mitochondrial protein with oncostatic activity. Our genetic and functional studies support a potential key role for MITOSTATIN in the development and progression of cancer.

Results

Cloning and characterization of MITOSTATIN

Using differential hybridization of cDNA libraries (subtractive hybridization) with probes obtained from logarithmically-growing or growth-suppressed cells (i.e.: decorin-transfected tumor cells), we isolated different growth-regulated genes. Northern blot of one of these

novel transcripts showed a 10-fold induction in three different decorin-transfected cells (A431, HeLa, and HT1080 cells), recognizing a transcript of ~3.2 Kb (data not shown). The difference in the MITOSTATIN protein levels between the clone and the parental line was confirmed by immunoblotting analysis (Figure S*1*). At the time of the cloning homology searches against EST databases showed complete identity with a published human EST. Human testis and skeletal muscle cDNA libraries were screened and 3'/5' RACE PCR performed to clone the 3.2-Kb full length cDNA including a 1,497 bp open reading frame containing a starting ATG codon at position 216 within a perfect Kozak consensus sequence that we called *MITOSTATIN* (deposited in the GeneBank™ with accession number AY007230). The entire human *MITOSTATIN* spans 17 Kb of genomic DNA, with thirteen exons, twelve of which were coding exons (Figure 1a). Search analysis against available protein databases identified *Pan troglodytes*, *Pongo Pygmaeus*, *Canis familiaris*, *Bos Taurus*, *Mus musculus*, and *Rattus norvegicus* proteins with high homology (>80%) with the *MITOSTATIN* ORF, indicating that it is highly conserved in mammals (Figure 1b and Figure S*2*).

Expression of human MITOSTATIN

MITOSTATIN expression in normal human tissues was examined using two multiple normal-tissue Northern blots. All tissues examined (brain, heart, skeletal muscle, colon, thymus, spleen, kidney, liver, small intestine, placenta, lung, peripheral blood leucocyte, prostate, testis, and ovary) demonstrated the presence of the 3.2 Kb MITOSTATIN transcript, albeit at different levels. The highest RNA expression was detected in heart, skeletal muscle, kidney, liver, and testis. A larger 5.5 Kb transcript was observed in heart and skeletal muscle. A smaller RNA transcript of 1.24 Kb was also detected in heart mRNA (Figure 1c).

To determine whether the wild-type *MITOSTATIN* cDNA could be translated *in vitro*, we performed *in vitro* transcription/translation by a TnT-coupled reticulocyte system. Analysis of the synthesized protein by SDS-polyacrylamide gel electrophoresis (SDS-PAGE) and autoradiography confirmed the 61.2 kDa predicted protein (Figure S*4*). To assess whether *MITOSTATIN* cDNA could be translated *in vivo*, full length *MITOSTATIN* was cloned in pcDNA3.1 Myc/His vector. Western blot analysis of the fusion protein in HeLa and 293T transfected cells showed presence of the MITOSTATIN protein around 62 kDa.

Next, we determined the sub-cellular localization of this newly identified gene product to gain insights into its function. Various expression vectors harboring *MITOSTATIN* with GFP located at the N- or C-terminal ends, or with FLAG epitopes at the C-terminus were generated and tested in transient cell transfection assays in HeLa cells. In all cases, MITOSTATIN exhibited punctuate vesicular distribution throughout the cytoplasm (Figure 2a). Next, we discovered that MITOSTATIN, co-localized with mitochondrial markers (Figure 2b). To corroborate this subcellular distribution, we employed subcellular fractionation and immunoblotting of the various fractions. The results showed that MITOSTATIN specifically sedimented in the heavy mitochondrial fraction together with cytochrome C (Figure 2c). Similar results were obtained in embryonic kidney 293T cells and prostate cancer derived cell lines PC3, and LNCaP (Figure S*5*). We did not detect any

co-localization of MITOSTATIN with lysosomes, Golgi apparatus, or endosomal compartment (Figure S*6*). These results clearly show that MITOSTATIN is a novel mitochondria-associated protein.

MITOSTATIN interferes on mitochondria morphology and ultrastructural organization

Because of confocal images of subcellular localization suggested that MITOSTATIN protein is localized at the mitochondrial level, we analyzed MITOSTATIN effect on normal mitochondrial morphology. Mitochondrial shape results from the balance between fusion and fission, regulated by a family of "mitochondria-shaping" proteins impinging on both sides of the equilibrium. Core components in mammals include the pro-fusion proteins optic atrophy 1, mitofusins 1 and 2; and the pro-fission ones Fis1 and dynamin related protein 1 (Drp1) (Cereghetti *et al.*, 2006). We wished to verify if high levels of MITOSTATIN were associated with changes in normal mitochondrial morphology. To this end we expressed a mitostatin-V5 fusion protein together with the fluorescent protein dsRED targeted to the mitochondrial matrix (mt-dsRED) (Dimmer *et al.*, 2008) and acquired confocal images of the mitochondrial reticulum in HeLa cells (Figure 3a–d). High levels of MITOSTATIN induced marked changes in mitochondrial morphology, including fragmentation of the highly branched network of HeLa cells and clumping of the fragmented organelles in the perinuclear region. Since mitochondrial fragmentation can depend on the activation of the core fission machinery, we tested if a dominant negative mutant of Drp1 could interfere with the observed changes. The dominant negative $Drp1^{K38A}$ (Smirnova *et al.*, 1998) further elongated the mitochondrial network of HeLa cells and it blocked fragmentation induced by MITOSTATIN, as further confirmed by a morphometric analysis (Figure 3e). However, $Drp1^{K38A}$ had no effect on perinuclear clusterization of mitochondria observed in cells expressing high levels of MITOSTATIN, suggesting that the two observed phenotypes can be functionally dissected. Of note, since these experiments were carried in the presence of the broad caspase inhibitor zVAD-fmk, it is unlikely that the observed changes reflect the activation by MITOSTATIN of the apoptotic cascade, often associated with mitochondrial fragmentation and clustering. In conclusion, fragmentation induced by MITOSTATIN depends on the core mitochondrial fission machinery, while it can induce perinuclear clustering of the organelle occur when fission is blocked.

To further investigate MITOSTATIN's relationship with mitochondria, we analyzed wild type PC3 prostate carcinoma derived cells and PC3 MITOSTATIN-over-expressing clones (PC3 B2) by transmission electron microscopy (TEM). Ultrastructural analysis of MITOSTATIN-over-expressing PC3 cells revealed that the mitochondria were often round and showed abnormal christae in contrast to the wild-type cells (Figure 4a). In addition, mitochondria were often swollen and lost some of their christae and matrix material (Figure 4b and 4c).

De novo expression of MITOSTATIN inhibits cell growth

We hypothesized that MITOSTATIN could be linked to growth control insofar as it was a decorin-induced gene. Therefore, we utilized the *MITOSTATIN*-GFP constructs described above to test their biological activity in transformed cells. MITOSTATIN expression significantly affected HeLa colony formation, with a drastic reduction (65%) in the number

and size of colonies as compared to vector-transfect controls (Figure 5a, $P<0.05$, n=3). Confocal microscope analysis demonstrated that the *MITOSTATIN*-GFP colonies were indeed derived from cells not expressing MITOSTATIN, as shown by absence of green fluorescence (Figure 5b). Comparably, the rate of DNA synthesis in HeLa and 293T cells decreased by 83% and 60%, respectively (Figure 5c–d, $P<0.01$).

To further investigate the MITOSTATIN effects on tumor cell growth, we transfected PC3, LNCaP, and 5637 cells with a *MITOSTATIN*-V5 fusion expression construct, and PC3 and DU145 cells with an anti-sense cDNA construct. Moreover, we placed *MITOSTATIN* in a self-inactivating retroviral vector under the control of an inducible *Drosophila* HSP70 promoter, that we used to transfect DU145 cells. We obtained five clones stably over-expressing MITOSTATIN and two clones which showed a decreased level of endogenous MITOSTATIN (Figure 6a and b). Clones showed different levels of the protein over-expression: in PC3 cells, PC3 B2 had a 2.0 fold increase over parental cells; DU145-MITOSTATIN showed a 4.2 fold increase; in LNCaP clones, LNCaP B1A, LNCaP B3A and LNCaP A3A had a 1.6, 2.1 and 2.6 fold increase, respectively; 5637 B3 MITOSTATIN expression was 2.9 times over the parental cells expression.

As observed in transiently-transfected clones, MITOSTATIN over-expressing clones showed a statistically significant reduction in cell number when compared with control vector and parental cells after 72 h (Figure 6c, n=3). Antisense clones PC3 M2 and DU145 M2 did not show a statistically-significant growth increase in comparison to control cells (p=ns, n=3).

A link between MITOSTATIN, Hsp27 expression and apoptosis

Next, we determined whether MITOSTATIN would affect apoptosis. To this end, we treated various tumor cell lines with staurosporine (1μM for 4 h), an established inducer of apoptosis (Mehlen *et al.*, 1996). Because several MAPKs are involved in the control of the apoptotic process, we tested the activation of several proteins in the Akt and Jnk kinase pathways after induction of apoptosis by staurosporine treatment (data not shown). We discovered that the phosphorylation of Hsp27 at Ser^{82} was specifically and uniquely inhibited by MITOSTATIN overexpression (Figure 7c). Moreover, Hsp27 levels were inversely proportional to levels of MITOSTATIN expression in prostate cancer cell lines (Figure 6b and Figure 7c). Remarkably, Hsp27 decreased in LNCaP B1A, B3A and A3A MITOSTATIN over-expressing clones, and its level was higher than in the parental cells when MITOSTATIN expression was abrogated with antisense mRNA in clones PC3 M2 and DU145 M2 (Figure 6b). In all cases, the MITOSTATIN-overexpressing cells showed a significant increase in apoptotic rate as compared to the low expressors (Figure 7a, $P<0.05$, n=3). The enhanced pro-apoptotic activity of MITOSTATIN-over-expressing clones was further confirmed by FACS analysis (Figure 7b). Notably, MITOSTATIN over-expression caused an enhanced inhibition of Hsp27-$PSer^{82}$ and Hsp27-$PSer^{78}$ (Figure 7c). A similar effect on Hsp27 phosphorylation was also observed after treatments with H_2O_2, TNF-α and actinomycin D, three established inducers of apoptosis, in LNCaP and PC3 cell lines (data not showed). Collectively, our findings indicate that MITOSTATIN is involved in facilitating cancer cells death upon apoptotic stimuli.

MITOSTATIN is mutated in various transformed cell lines and its expression can be lost in tumor samples

To determine whether *MITOSTATIN* is mutated or lost in malignant human tumors, we performed a systematic analysis of cancer-derived cell lines and solid tumors using RT-PCR. *MITOSTATIN* mRNA was absent in ~6% of the cancer samples (1 vulva, 2 colon and 3 prostate cancers; 4.2% including the cancer cell lines). Also in the three prostate samples, we studied the normal counterpart in which the gene was normally expressed (Figure 8a). Four point mutations were detected (Figure S8). In the gastric carcinoma derived RF48 cell line, T345 in exon 2 was substituted in heterozygosity by a C, changing the aminoacid from a serine to a proline (S44P). In the prostate derived LNCaP cell line, C 184 in exon 9 was substituted in heterozygosity by a T, without aminoacid changes (A323A). In the pancreatic carcinoma derived SU86 cell line, G 890 in exon 6 was substituted in heterozygosity by an A, without changing the glutamic acid (E225E). In the CAPAN1 pancreatic carcinoma derived cells, C 492 in exon 3 was homozygously mutated to A, changing the aminoacid from glutamic acid to lysine (E93K). Notably, all these mutations affected aminoacid residues that are highly conserved in evolution (Figure 1c and Figure S8). In immunofluorence confocal analysis MITOSTATIN still showed a punctuate pattern of distribution and co-localized within mitochondria in LNCaP (Figure S5), CAPAN and Su86.

Reduced MITOSTATIN expression in advanced bladder and breast carcinomas

To further confirm our hypothesis on the tumor suppressive nature of MITOSTATIN, we evaluated its expression in a series of bladder and breast cancers by immunohistochemistry. In normal samples, high MITOSTATIN levels were detected in normal urothelial and breast epithelial cells (Figure 8b–c, Figure S9). Also, as expected from the RNA analysis (Figure 1), MITOSTATIN protein was readily detected in smooth muscle and endothelial cells (Figure 8b). MITOSTATIN was mainly localized into the cytoplasm, in agreement with the mitochondrial nature detected by transient expression. Interestingly, in normal mammary glands a strong MITOSTATIN signal was detected in both cytoplasm and cell membrane. In contrast, 22% (10/45) of bladder cancers did not show any MITOSTATIN expression. Univariate analysis revealed a decreased MITOSTATIN immunohistochemical score associated with advanced tumor stage (P=0.003) (Figure 8c) and higher pT (P=0.003). By multivariate analysis, the same variables were independently associated with MITOSTATIN immunohistochemical levels (Stage P=0.005; pT P=0.004). Approximately 23% (11/48) of the breast tumors did not express MITOSTATIN. In the univariate analysis, a decreased MITOSTATIN immunohistochemical score correlated to advanced tumor stage (P=0.047) (Figure 8c), and higher pT (P=0.027). In breast tumors, lower MITOSTATIN immunohistochemical expression was also associated, although not with statistical significance, with presence of lymph node metastases (P=0.053). There was no statistically-significant association between MITOSTATIN expression and estrogen receptor and progesterone receptor status, histologic and nuclear grade, and tumor histotype (data not shown). No other clinical-pathological parameters resulted independently associated to MITOSTATIN expression in breast cancers in the multivariate analysis.

Discussion

Previous reports of allelic loss at chromosome 12q24 in solid tumors have identified frequencies ranging from 25–55% depending on marker sets used for LOH studies (Aubele *et al.*, 2000; Field *et al.*, 1995; Jiang *et al.*, 1998; Kimura *et al.*, 1998; Koo *et al.*, 1999; Rijken *et al.*, 1999; Sattler *et al.*, 1999; Schmutte *et al.*, 1997; Shiseki *et al.*, 1996; Tirkkonen *et al.*, 1997). Interestingly, an RFLP study showed that deletions at 12q24 were more frequent in brain metastases (68% of LOH) of lung cancers than in stage I lung tumors (29% to 33% of LOH). In accordance with this report, a CGH analysis on two microdissected breast carcinomas showed amplification of the central portion of chromosome 12 in the primary tumors and LOH at 12q24 in one metastatic lymph-node (Aubele *et al.*, 1999). We have previously suggested that thymine-DNA glycosylase (TDG), an enzyme initiating T:G mismatch repair by specifically excising T from those mismatches through a glysosylase mechanism in C→T transitions, may be a good tumor suppressor candidate for 12q24 deletions. To test our hypothesis, we first characterized the structure of the *TDG* gene and selected 10 out of 24 (42%) gastric carcinomas with LOH at the *TDG* locus. Nevertheless, although gastric cancer presents a high percentage of C→T transitions, we found no mutations within the coding sequence of the remaining *TDG* allele in the gastric samples that displayed LOH (Schmutte *et al.*, 1997). According to these results, we suggested that a gene different than *TDG* is the target of 12q24 deletions. In this study, we describe the identification and functional characterization of a novel putative tumor suppressor gene, *MITOSTATIN*, at 12q24.1 and show that *MITOSTATIN* has many of the hallmarks of a typical tumor suppressor gene.

First we show that MITOSTATIN is expressed, although at different levels, in all the human tissues we tested and that it co-localizes to the mitochondria, affecting mitochondria morphology and ultrastructural organization. Second, we show that MITOSTATIN significantly inhibits colony formation and evokes a dramatic reduction in the rate of DNA synthesis in various transformed cell lines. Third, MITOSTATIN over-expression is pro-apoptotic. Fourth, there is a direct correlation between the amount of intra-cellular MITOSTATIN protein and its biological effects: all MITOSTATIN-over-expressing cells show a lower growth rate, whereas cells over-expressing an anti-sense MITOSTATIN mRNA grow at a slight higher rate than parental cells.

A previous report (Nishizawa *et al.*, 2005) indicated that MITOSTATIN is a cytoplasmic protein that co-localizes with keratin filaments and was therefore named trichoplein. However, our findings although did not exclude the interaction with keratins, clearly show that MITOSTATIN associates with mitochondria even if it should be stressed that the association is not complete, the localization of the protein is on the outer membrane and that other unidentified intracellular structures are stained by anti-MITOSTATIN antibodies. Moreover, fusion to GFP of different fragments of MITOSTATIN showed that the first 111 amino acids are sufficient for a punctuate distribution that partially overlaps with mitochondria (VA and LS, unpublished data). The co-localization of MITOSTATIN with mitochondria (here) as well as with keratin filaments (Nishizawa *et al.*, 2005) could rise the hypothesis that this protein regulates interaction of the organelle with the intermediate filaments, a process which impacts on movement and subcellular localization of the

organelle (Anesti and Scorrano, 2006). In fact, high levels of MITOSTATIN are associated with changes in the shape of the mitochondrial network, with a remarkable fragmentation and perinuclear clustering. While the former depends on the activation of the core fission machinery, the latter occurs independently of it, as substantiated by the lack of inhibition by a dominant negative Drp1. The clusterization phenotype is typical of apoptotic cells, as observed in the late nineties in TNFα-treated fibroblasts (De Vos *et al.*, 1998), as well as of cells over-expressing hFis1, the mitochondrial receptor for Drp1 (Frieden *et al.*, 2004). We could rule out not only that in our case it depended on Drp1, but also that it was an epiphenomenon of the pro-apoptotic action of MITOSTATIN, given the lack of inhibition by the caspase inhibitor zVAD-fmk. It is possible that the perinuclear clusterization reflects the hijack of mitochondria from microtubules to intermediate filaments, which MITOSTATIN can bind to (Nishizawa *et al.*, 2005).

The mitochondrial localization would also explain its potential involvement in apoptosis. Mitochondria are central organelles in the regulation of apoptosis, mainly by amplifying death signals via the release of cytochrome c and other protein cofactors from the inter-membrane space to the cytosol, where they activate effector caspases. The mechanisms by which increased expression of MITOSTATIN facilitates apoptosis remain to be resolved, but it is conceivable that this occurs via a facilitator effect on the mitochondrial pathway of apoptosis.

In this study we discover a link between MITOSTATIN expression and Hsp27 phosphorylation. Hsp27 is a heat shock protein and in quiescent cells exists predominantly as a large oligomeric unit of ~800 kDa. During stress, the level of Hsp27 and the amount of phosphorylation on Ser 15, 78 and 82 increases, resulting in a shift in Hsp27 from an oligomeric unit to tetrameric and dimeric units (Bruey *et al.*, 2000). Hsp27 has cytoprotective effects during cellular stress and operates as a molecular chaperone inhibiting protein unfolding. Hsp27 also directly interferes with caspase activation, modulates oxidative stress and regulates the cytoskeleton scaffolding (Parcellier *et al.*, 2003). Higher levels of Hsp27 have been correlated with an increased metastatic potential of tumor cells *in vitro* and *in vivo* as well as an enhanced resistance to therapy (Kamada *et al.*, 2007). Hsp27 has been frequenly detected over-expressed in human cancer (Cornford *et al.*, 2000; Ehrenfried *et al.*, 1995; Langdon *et al.*, 1995; Lebret *et al.*, 2003; Love and King, 1994; Takashi *et al.*, 1998). Specifically in prostate cancer, elevated Hsp27 expression has been linked to hormone resistance and poor outcome (Rocchi *et al.*, 2005; Rocchi *et al.*, 2004). Thus, MITOSTATIN-evoked effects on Hsp27 phosphorylation might be directly linked to MITOSTATIN ability to inhibit cell growth and be pro-apoptotic during cell stress.

The loss of tumor suppressor gene regulatory function represents an important step in malignant progression (Hanahan and Weinberg, 2000). Mutations of tumor suppressor genes are considered recessive, and both copies of these genes must be inactivated before the cell is at risk of transformation, the so-called “two hit” hypothesis (Knudson, 2000). The heterozygous situation, in which only one allele is not functioning, may cause a reduced action of the gene (haploinsufficiency) and favors the development of the neoplastic phenotype. Therefore, after we determined that *MITOSTATIN* is localized in a chromosomal region deleted in cancer and that its expression is induced by decorin, a cancer-cell growth

inhibitor (Iozzo, 1998), we performed a mutational analysis in cell lines and primary human tumors of different origin. Approximately 6% of the cancer samples analyzed show homozygous deletions of the *MITOSTATIN* gene. In three primary human prostate cancers, we showed that the *MITOSTATIN* mRNA was normally expressed in the normal adjacent glands. Three of the four point mutations present in cancer cell lines (RF48 gastric carcinoma derived cell line, prostate cancer LNCaP cell line, and pancreatic carcinoma derived SU86 cell line) were detected in one of the two *MITOSTATIN* alleles together with the normal allele. *MITOSTATIN* was homozygously mutated in the CAPAN1 pancreatic carcinoma derived cells. The low incidence of *MITOSTATIN* mutations suggests that other molecular mechanisms are responsible for the loss of expression of MITOSTATIN observed in primary tumors. The presence of mutations in only one of the two alleles also suggests that *MITOSTATIN* could also be a haploinsufficient tumor suppressor.

Several reports have suggested that 12q24 contains a tumor suppressor gene involved in multiple tumor types (Aubele *et al.*, 2000; Field *et al.*, 1995; Jiang *et al.*, 1998; Kimura *et al.*, 1998; Koo *et al.*, 1999; Rijken *et al.*, 1999; Sattler *et al.*, 1999; Schmutte *et al.*, 1997; Shiseki *et al.*, 1996; Tirkkonen *et al.*, 1997). We mapped the *MITOSTATIN* gene to this region and showed a loss of *MITOSTATIN* RNA expression in several carcinomas. Although, the status of DNA and RNA is important, the actual determinant of a gene function is its protein expression. Using immunohistochemistry experiments, we showed that MITOSTATIN protein is absent or greatly reduced in 22% of human bladder cancers and 23% of breast adenocarcinomas. Loss of MITOSTATIN expression correlates with advanced disease in both type of cancer. Furthermore, it was associated with lymph-node metastases in breast cancer. These *in vivo* data represent an additional evidence of the possible tumor suppressor function of MITOSTATIN.

In conclusion, we have identified and functionally characterized MITOSTATIN, a novel putative tumor suppressor gene localized to the mitochondria. We further provide the first evidence that loss of MITOSTATIN protein expression may play a role in human tumorigenesis. Thus, loss of function of MITOSTATIN may interrupt the inhibitory circuit, possibly regulated by extracellular components such as decorin, facilitating the growth and spread of neoplastic cells.

Our findings support the hypothesis that MITOSTATIN behaves as a classical tumor suppressor in solid tumors. Furthermore, we demonstrate, for the first time, that MITOSTATIN is implicated in the control of cell growth and apoptosis and that MITOSTATIN protein is significantly decreased or absent in advanced bladder and breast cancers. It remains to be determined how MITOSTATIN functions in mitochondrial homeostasis as well as how a mitochondrial protein acts as tumor suppressor. Additional functional studies are needed to clarify the role of this protein in neoplastic transformation, and the mechanisms of MITOSTATIN inactivation.

Materials and Methods

Materials

Additional details of materials are provided in Supplementary Information

Tissue samples

A total of 102 (26 matched normal and tumor tissues) de-identified frozen primary tumors were collected from 1994 to 2000 from archives of the Pathology Department of Thomas Jefferson University. Samples studied included 31 bladder, 23 colon-rectum, 20 prostate, 13 ovary, 13 vulva and 2 cervical cancers. All samples were obtained from patients who gave informed consent to use excess pathological specimens for research purposes. The AccuMax Array-A215 (Accumax Array) including 94 0.6-mm bladder cancer cores was utilized for the immunohistochemistry. Forty-eight invasive breast carcinomas (41 ductal and 7 lobular) were selected from the Pathology Tissue Bank of Thomas Jefferson University and used to develop a tissue microarray based upon the appropriate IRB approved protocol. Adjacent normal breast from four diseased patients was also included.

Cell proliferation, colony formation assays and subcellular fractionation

Cells were plated in triplicate in a 6-well tissue culture plate. Proliferation was assessed by counting the cells daily for four days, and the mean values of three independent experiments were analyzed. Colony forming assay was performed on cells plated at a density of 400 cells/100 mm dish. On day 15, cells were fixed with PBS-3.7% formaldehyde and stained with crystal violet for colony counting. Separation of crude organelle fractions was performed on cell using the differential centrifugation methods (Bourgeron *et al.*, 1992; Peruzzi *et al.*, 1999) with minor modifications.

Generation of MITOSTATIN polyclonal antibody and immunological analyses

The anti-MITOSTATIN antibody was raised in rabbit against glutathione 6HIS-fusion MITOSTATIN protein corresponding to nucleotides 816–1712, which was expressed in *Escherichia coli* and purified with a fusion tag column. Protein extraction and immunoblot analyses were done as described previously (Vecchione *et al.*, 2002). Anti-MITOSTATIN (1:1,000), anti-actin (1:10,000) (Sigma), anti-FLAG (1:1,000) (Sigma), anti-Cytochrome-C (1:1,000) (Cell Signaling), anti-caspase-3 (1:1,000) (BD Pharminen Inc.), anti-PARP (1:1,000) (BD Pharmingen Inc.), anti-HSP27 (1:1,000) (Cell Signaling), anti-p38 MAP Kinase (1:1,000) and the phosphorylated anti-phospho-HSP27 ser82 (1:1,000), anti-phospho-HSP27 ser78 (1:1,000)) and anti-phospho-p38 MAPK thr180/tyr182 (1:1000) were used as primary antibodies. Immunofluorescence experiments were carried out on fixed cells as described before (Monami *et al.*, 2006).

Immunohistochemistry

In this study we used the immunohistochemistry procedure described previously (Vecchione *et al.*, 2002) with minor modifications. Sections were immunostained overnight at RT with a 1:100 dilution of the anti-MITOSTATIN antibody. The primary antibody was omitted and replaced with pre-immune serum in the negative control. All sections were examined independently by two investigators (R.B., J.P.P.), and complete agreement was reached for MITOSTATIN positivity and negativity. Positive staining of anti-MITOSTATIN antibody was semiquantified with a four-tier system: +++, 67–100% MITOSTATIN-positive cells; ++, 34–66% MITOSTATIN-positive cells; +, 5–33% MITOSTATIN-positive cells; and 0, the tumors in which >95% of cells did not express MITOSTATIN.

Statistical Analysis

Statistical analysis was carried out with SigmaStat for Windows version 3.10 (Systat Software). All values were expressed as mean ± SE. Differences between means were evaluated with double sided *Z* test. The χ^2 test was used to examine the categorical variables and the association between MITOSTATIN immunohistochemical expression levels and other clinicopathological variables in univariate analysis. To identify variables independently associated to MITOSTATIN immunohistochemical levels, backward selection multivariate analysis was performed using the logistic regression model. Differences were considered statistically significant at $P<0.05$.

Supplementary Material

Refer to Web version on PubMed Central for supplementary material.

Acknowledgments

We thank Florencia Bullrich for the FISH analysis, Jonathan Brody for providing CAPAN1 cells and Jason Zoeller for help with the phylogenetic tree. Dr. Scorrano is a Senior Scientist of the Dulbecco-Telethon Institute. GenBank = GenBank Accession Number AY007230. NCBI Protein Database = NCB Accession Number AAG12971. This work was in part supported by the Sidney Kimmel Foundation for Cancer Research, the Benjamin Perkins Bladder Cancer Fund and the Martin Greitzer Fund (to R.B.), by Telethon Italy and AIRC Italy (to L.S.), the National Institutes of Health grants RO1 CA39481, RO1 CA47282 and RO1 CA120975 (to R.V.I.), RO1 DK068419 (to A.M.).

References

Anesti V, Scorrano L. The relationship between mitochondrial shape and function and the cytoskeleton. Biochim Biophys Acta. 2006; 1757:692–699. [PubMed: 16729962]

Aubele M, Mattis A, Zitzelsberger H, Walch A, Kremer M, Hutzler P, et al. Intratumoral heterogeneity in breast carcinoma revealed by laser-microdissection and comparative genomic hybridization. Cancer Genet Cytogenet. 1999; 110:94–102. [PubMed: 10214356]

Aubele MM, Cummings MC, Mattis AE, Zitzelsberger HF, Walch AK, Kremer M, et al. Accumulation of chromosomal imbalances from intraductal proliferative lesions to adjacent in situ and invasive ductal breast cancer. Diagn Mol Pathol. 2000; 9:14–19. [PubMed: 10718208]

Bourgeron T, Chretien D, Rotig A, Munnich A, Rustin P. Isolation and characterization of mitochondria from human B lymphoblastoid cell lines. Biochem Biophys Res Commun. 1992; 186:16–23. [PubMed: 1321601]

Bruey JM, Paul C, Fromentin A, Hilpert S, Arrigo AP, Solary E, et al. Differential regulation of HSP27 oligomerization in tumor cells grown in vitro and in vivo. Oncogene. 2000; 19:4855–4863. [PubMed: 11039903]

Cereghetti GM, Scorrano L. The many shapes of mitochondrial death. Oncogene. 2006; 25:4717–4724. [PubMed: 16892085]

Cornford PA, Dodson AR, Parsons KF, Desmond AD, Woolfenden A, Fordham M, et al. Heat shock protein expression independently predicts clinical outcome in prostate cancer. Cancer Res. 2000; 60:7099–7105. [PubMed: 11156417]

Csordas G, Santra M, Reed CC, Eichstetter I, McQuillan DJ, Gross D, et al. Sustained down-regulation of the epidermal growth factor receptor by decorin. A mechanism for controlling tumor growth in vivo. J Biol Chem. 2000; 275:32879–32887. [PubMed: 10913155]

De Vos K, Goossens V, Boone E, Vercammen D, Vancompernolle K, Vandenabeele P, et al. The 55-kDa tumor necrosis factor receptor induces clustering of mitochondria through its membrane-proximal region. J. Biol. Chem. 1998; 273:9673–9680. [PubMed: 9545301]

Dimmer KS, Navoni F, Casarin A, Trevisson E, Endele S, Winterpacht A, et al. LETM1, deleted in Wolf Hirschhorn syndrome is required for normal mitochondrial morphology and cellular viability. Hum Mol Genet. 2008; 17:201–214. [PubMed: 17925330]

Ehrenfried JA, Herron BE, Townsend CM Jr. Evers BM. Heat shock proteins are differentially expressed in human gastrointestinal cancers. Surg Oncol. 1995; 4:197–203. [PubMed: 8528482]

Field JK, Kiaris H, Risk JM, Tsiriyotis C, Adamson R, Zoumpourlis V, et al. Allelotype of squamous cell carcinoma of the head and neck: fractional allele loss correlates with survival. Br J Cancer. 1995; 72:1180–1188. [PubMed: 7577465]

Frieden M, James D, Castelbou C, Danckaert A, Martinou JC, Demaurex N. Ca^{2+} homeostasis during mitochondrial fragmentation and perinuclear clustering induced by hFis1. J. Biol. Chem. 2004; 279:22704–22714. [PubMed: 15024001]

Goldoni S, Iozzo RA, Kay P, Campbell S, McQuillan A, Agnew C, et al. A soluble ectodomain of LRIG1 inhibits cancer cell growth by attenuating basal and ligand-dependent EGFR activity. Oncogene. 2007; 26:368–381. [PubMed: 16847455]

Hanahan D, Weinberg RA. The hallmarks of cancer. Cell. 2000; 100:57–70. [PubMed: 10647931]

Iozzo RV. Matrix proteoglycans: from molecular design to cellular function. Annu Rev Biochem. 1998; 67:609–652. [PubMed: 9759499]

Jiang F, Richter J, Schraml P, Bubendorf L, Gasser T, Sauter G, et al. Chromosomal imbalances in papillary renal cell carcinoma: genetic differences between histological subtypes. Am J Pathol. 1998; 153:1467–1473. [PubMed: 9811338]

Kamada M, So A, Muramaki M, Rocchi P, Beraldi E, Gleave M. Hsp27 knockdown using nucleotide-based therapies inhibit tumor growth and enhance chemotherapy in human bladder cancer cells. Mol Cancer Ther. 2007; 6:299–308. [PubMed: 17218637]

Kimura M, Furukawa T, Abe T, Yatsuoka T, Youssef EM, Yokoyama T, et al. Identification of two common regions of allelic loss in chromosome arm 12q in human pancreatic cancer. Cancer Res. 1998; 58:2456–2460. [PubMed: 9622089]

Knudson AG. Chasing the cancer demon. Annu Rev Genet. 2000; 34:1–19. [PubMed: 11092820]

Koo SH, Kwon KC, Ihm CH, Jeon YM, Park JW, Sul CK. Detection of genetic alterations in bladder tumors by comparative genomic hybridization and cytogenetic analysis. Cancer Genet Cytogenet. 1999; 110:87–93. [PubMed: 10214355]

Langdon SP, Rabiasz GJ, Hirst GL, King RJ, Hawkins RA, Smyth JF, et al. Expression of the heat shock protein HSP27 in human ovarian cancer. Clin Cancer Res. 1995; 1:1603–1609. [PubMed: 9815962]

Lebret T, Watson RW, Molinie V, O'Neill A, Gabriel C, Fitzpatrick JM, et al. Heat shock proteins HSP27, HSP60, HSP70, and HSP90: expression in bladder carcinoma. Cancer. 2003; 98:970–977. [PubMed: 12942564]

Love S, King RJ. A 27 kDa heat shock protein that has anomalous prognostic powers in early and advanced breast cancer. Br J Cancer. 1994; 69:743–748. [PubMed: 8142264]

Mehlen P, Schulze-Osthoff K, Arrigo AP. Small stress proteins as novel regulators of apoptosis. Heat shock protein 27 blocks Fas/APO-1- and staurosporine-induced cell death. J Biol Chem. 1996; 271:16510–16514. [PubMed: 8663291]

Monami G, Gonzalez EM, Hellman M, Gomella LG, Baffa R, Iozzo RV, et al. Proepithelin promotes migration and invasion of 5637 bladder cancer cells through the activation of ERK1/2 and the formation of a paxillin/FAK/ERK complex. Cancer Res. 2006; 66:7103–7110. [PubMed: 16849556]

Moscatello DK, Santra M, Mann DM, McQuillan DJ, Wong AJ, Iozzo RV. Decorin suppresses tumor cell growth by activating the epidermal growth factor receptor. J Clin Invest. 1998; 101:406–412. [PubMed: 9435313]

Nishizawa M, Izawa I, Inoko A, Hayashi Y, Nagata K, Yokoyama T, et al. Identification of trichoplein, a novel keratin filament-binding protein. J Cell Sci. 2005; 118:1081–1090. [PubMed: 15731013]

Parcellier A, Schmitt E, Gurbuxani S, Seigneurin-Berny D, Pance A, Chantome A, et al. HSP27 is a ubiquitin-binding protein involved in I-kappaBalpha proteasomal degradation. Mol Cell Biol. 2003; 23:5790–5802. [PubMed: 12897149]

Peruzzi F, Prisco M, Dews M, Salomoni P, Grassilli E, Romano G, et al. Multiple signaling pathways of the insulin-like growth factor 1 receptor in protection from apoptosis. Mol Cell Biol. 1999; 19:7203–7215. [PubMed: 10490655]

Rijken AM, Hu J, Perlman EJ, Morsberger LA, Long P, Kern SE, et al. Genomic alterations in distal bile duct carcinoma by comparative genomic hybridization and karyotype analysis. Genes Chromosomes Cancer. 1999; 26:185–191. [PubMed: 10502315]

Rocchi P, Beraldi E, Ettinger S, Fazli L, Vessella RL, Nelson C, et al. Increased Hsp27 after androgen ablation facilitates androgen-independent progression in prostate cancer via signal transducers and activators of transcription 3-mediated suppression of apoptosis. Cancer Res. 2005; 65:11083–11093. [PubMed: 16322258]

Rocchi P, So A, Kojima S, Signaevsky M, Beraldi E, Fazli L, et al. Heat shock protein 27 increases after androgen ablation and plays a cytoprotective role in hormone-refractory prostate cancer. Cancer Res. 2004; 64:6595–6602. [PubMed: 15374973]

Sambrook, JFE.; Maniatis, T. Molecular cloning: a laboratory manual. Plainview, NY: Cold Spring Harbor Lab. Press; 1989.

Santra M, Mann DM, Mercer EW, Skorski T, Calabretta B, Iozzo RV. Ectopic expression of decorin protein core causes a generalized growth suppression in neoplastic cells of various histogenetic origin and requires endogenous p21, an inhibitor of cyclin-dependent kinases. J Clin Invest. 1997; 100:149–157. [PubMed: 9202067]

Santra M, Skorski T, Calabretta B, Lattime EC, Iozzo RV. De novo decorin gene expression suppresses the malignant phenotype in human colon cancer cells. Proc Natl Acad Sci U S A. 1995; 92:7016–7020. [PubMed: 7624361]

Sattler HP, Rohde V, Bonkhoff H, Zwergel T, Wullich B. Comparative genomic hybridization reveals DNA copy number gains to frequently occur in human prostate cancer. Prostate. 1999; 39:79–86. [PubMed: 10221562]

Schmutte C, Baffa R, Veronese LM, Murakumo Y, Fishel R. Human thymine-DNA glycosylase maps at chromosome 12q22-q24.1: a region of high loss of heterozygosity in gastric cancer. Cancer Res. 1997; 57:3010–3015. [PubMed: 9230216]

Shiseki M, Kohno T, Adachi J, Okazaki T, Otsuka T, Mizoguchi H, et al. Comparative allelotype of early and advanced stage non-small cell lung carcinomas. Genes Chromosomes Cancer. 1996; 17:71–77. [PubMed: 8913723]

Smirnova E, Shurland DL, Ryazantsev SN, van der Bliek AM. A human dynamin related protein controls the distribution of mitochondria. J. Cell Biol. 1998; 143:351–358. [PubMed: 9786947]

Takashi M, Katsuno S, Sakata T, Ohshima S, Kato K. Different concentrations of two small stress proteins, alphaB crystallin and HSP27 in human urological tumor tissues. Urol Res. 1998; 26:395–399. [PubMed: 9879819]

Tirkkonen M, Johannsson O, Agnarsson BA, Olsson H, Ingvarsson S, Karhu R, et al. Distinct somatic genetic changes associated with tumor progression in carriers of BRCA1 and BRCA2 germ-line mutations. Cancer Res. 1997; 57:1222–1227. [PubMed: 9102202]

Vecchione A, Ishii H, Baldassarre G, Bassi P, Trapasso F, Alder H, et al. FEZ1/LZTS1 is down-regulated in high-grade bladder cancer, and its restoration suppresses tumorigenicity in transitional cell carcinoma cells. Am J Pathol. 2002; 160:1345–1352. [PubMed: 11943719]

Xu G, Guimond MJ, Chakraborty C, Lala PK. Control of proliferation, migration, and invasiveness of human extravillous trophoblast by decorin, a decidual product. Biol Reprod. 2002; 67:681–689. [PubMed: 12135914]

Abbreviations

LOH	loss of heterozygosity
PCR	polymerase chain reaction
GFP	green fluorescent protein

TUNEL	terminal deoxynucleotidyltransferase-mediated dUTP nick end-labeling
CGH	Comparative Genomic Hybridization
RFLP	Restriction Fragment Length Polymorphism

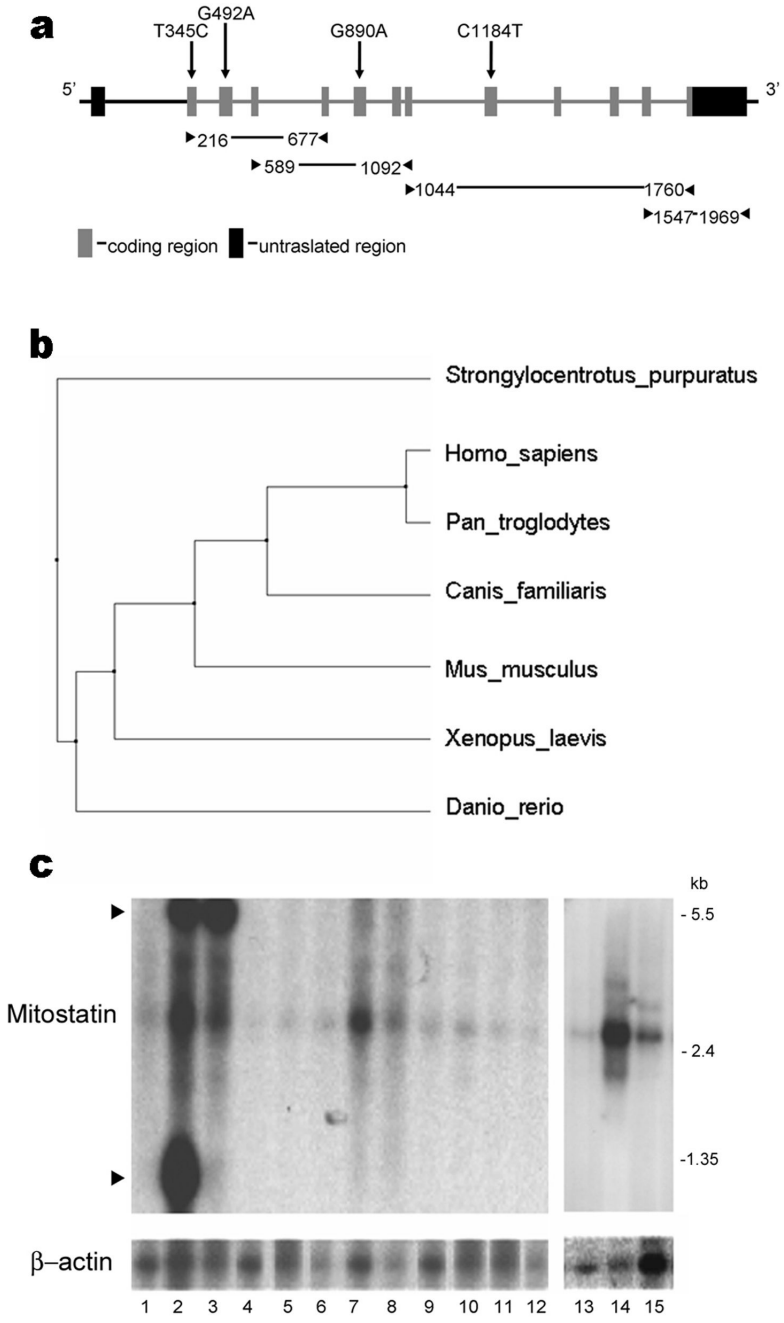

Figure 1. *MITOSTATIN* gene structure, homologies and expression in normal human tissues

(**a**) Schematic representation of the *MITOSTATIN* gene and distribution of primers along the *MITOSTATIN* transcript. Also the four point mutations detected in cancer cells are shown. Primer sets used in the RT-PCR study are numbered underneath. (**b**) Phylogenetic tree among different species of *MITOSTATIN* orthologs. (**c**) *MITOSTATIN* is ubiquitously expressed in normal human tissues as shown by Northern blot analysis on normal human tissue samples (1 = brain, 2 = heart, 3 = skeletal muscle, 4 = colon, 5 = thymus, 6 = spleen, 7

= kidney, 8 = liver, 9 = small intestine, 10 = placenta, 11 = lung, 12 = peripheral blood leucocyte, 13 = prostate, 14 = testis, and 15 = ovary). The β-actin RNA was used as control.

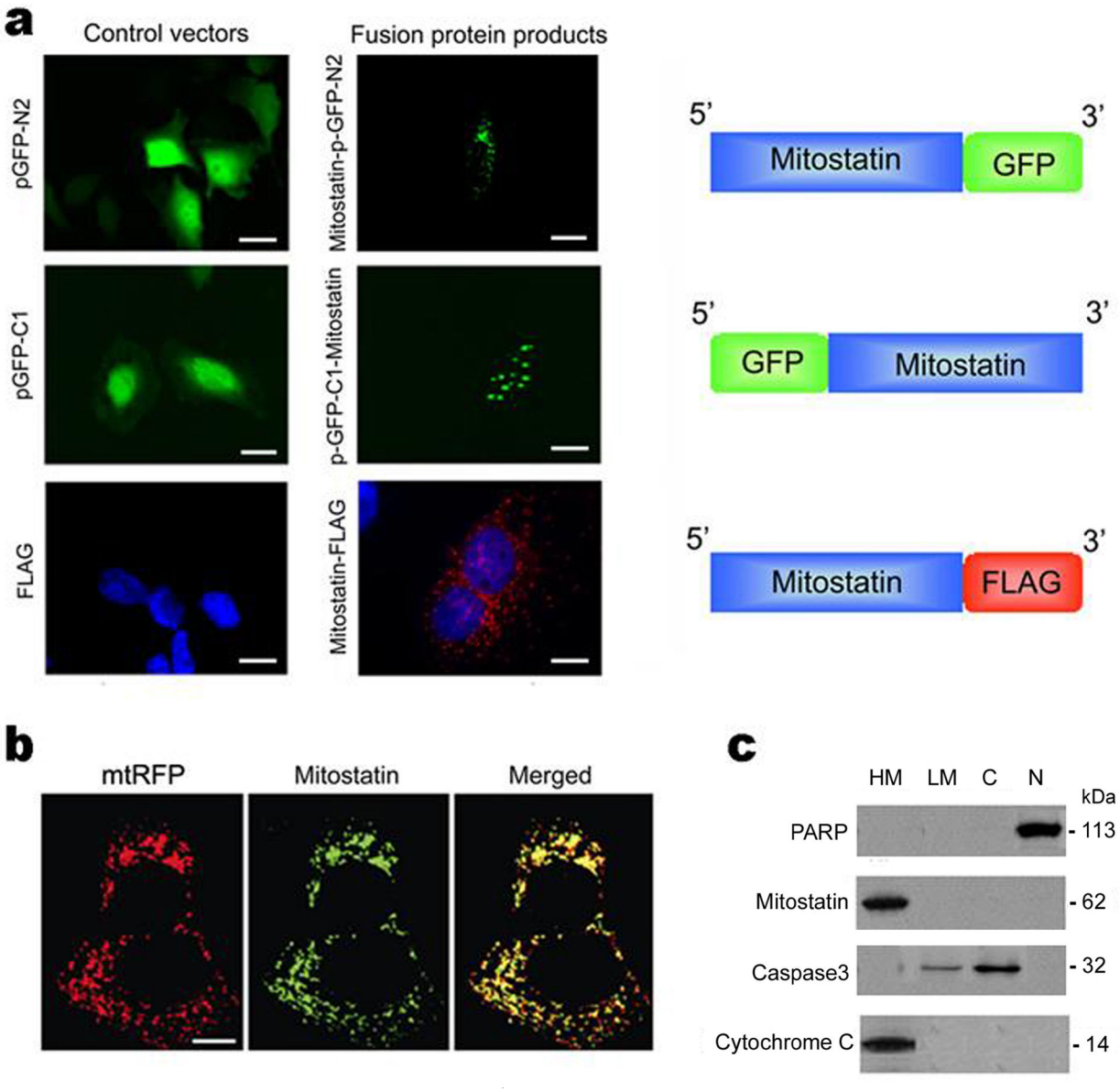

Figure 2. Subcellular localization of MITOSTATIN

(**a**) *MITOSTATIN* cDNAs fused with pEGFP-N2, pEGFP-C1, and FLAG exhibited punctuate vesicular distribution through the cytoplasm when transfected in HeLa cells. Bars, 20 μm. (**b**) Confocal images in HeLa cells of MITOSTATIN-*GFP* chimeric protein and mitochondrially targeted dsRED (mtRFP); merge shows a partial co-localization (*yellow*). Bar, 10 μm. (**c**) Western blot analysis using anti-FLAG antibody in HeLa cells revealed the presence of ~62 kDa band in the mitochondrial pellet fraction of the transfected (HM: heavy membranes; LM: light membranes; C: cytoplasm; N: nucleus). Antibodies specific for cytochrome *c* (mitochondrial marker), caspase-3 (cytosolic marker) and PARP (nuclear marker) were used to characterize the fractions.

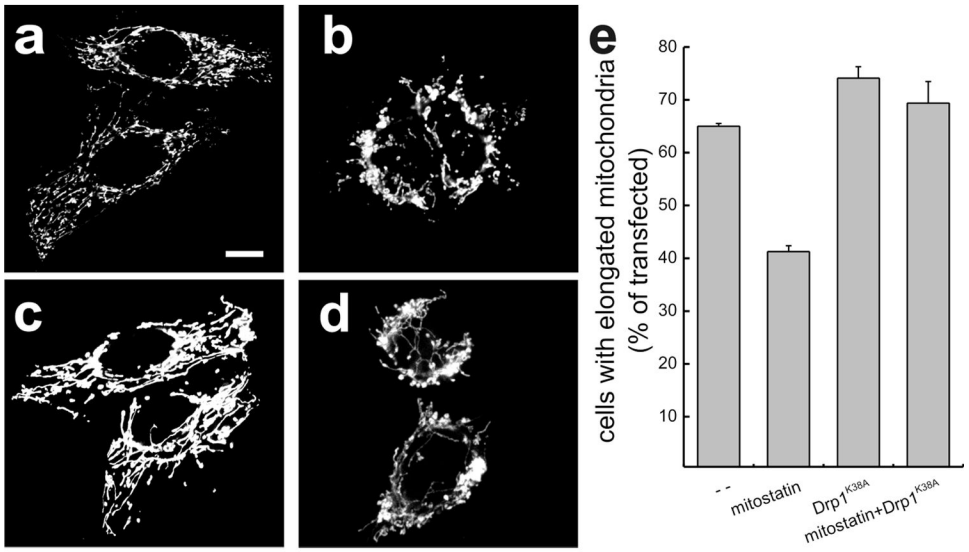

Figure 3. MITOSTATIN promotes mitochondrial fragmentation and clumping independently of Drp1

(**a–d**) Representative confocal images of mt-dsRED fluorescence in HeLa cells transfected with mt-dsRED (**a**) or co-transfected with mt-dsRED and MITOSTATIN (**b**), dominant negative Drp1 (Drp1^{K38A}, **c**), and MITOSTATIN plus Drp1^{K38A} (**d**). Bar, 10 μm. (**e**) morphometric analysis of mitochondrial fragmentation induced by overexpression of MITOSTATIN. Data represent mean ± SE of 5 independent experiments.

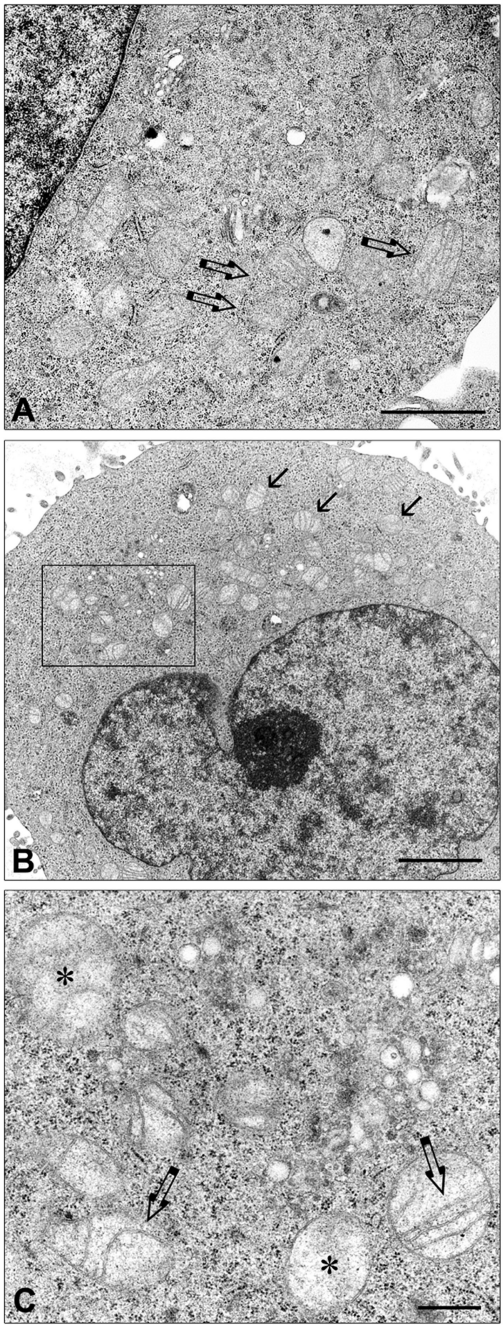

Figure 4. Ultrastructural analysis of MITOSTATIN-expressing PC3 prostate carcinoma cells show abnormal mitochondrial structure

(**a**) Electron micrograph of a wild-type PC3 cell shows normal appearing mitochondria (empty arrows). Bar, 2 μm. (**b**) Ultrastructural analysis of a MITOSTATIN-expressing cells. Note the large number of small, swollen mitochondria (black arrows). Bar, 2 μm. (**c**) High magnification of the inset in B shows loss of mitochondrial matrix (asterisks) and abnormal christae (empty arrows). *Bar*, 0.2 μm.

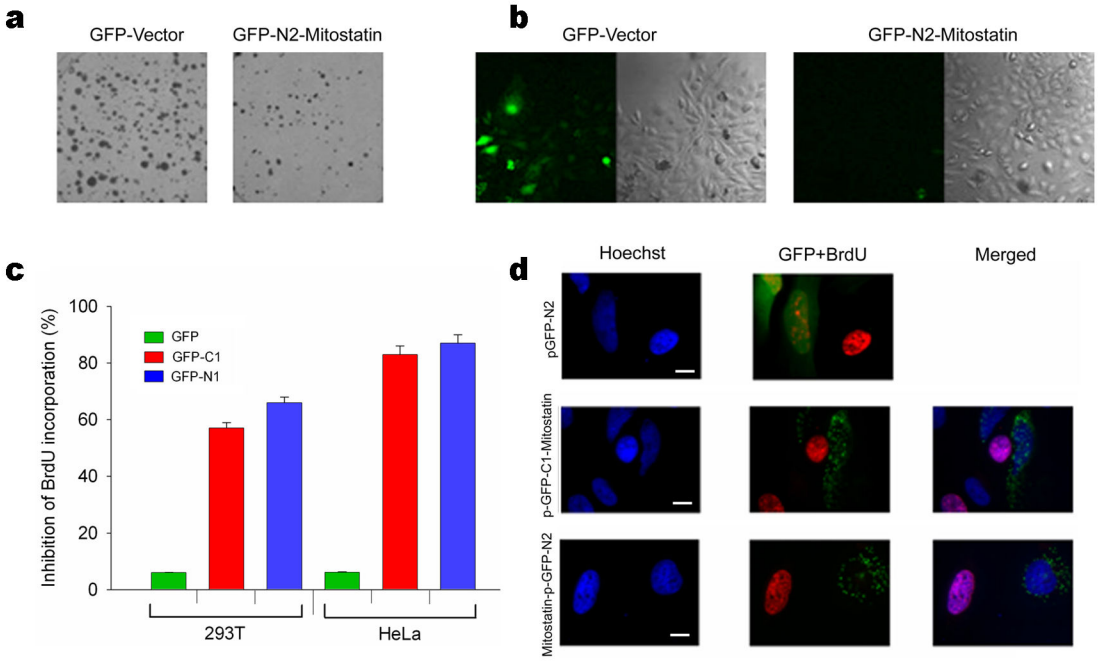

Figure 5. MITOSTATIN expression affects colony formation in HeLa cells and DNA syntesis in HeLa and 293 cell lines

(**a**) Forty-eight h after transfection, MITOSTATIN expression significantly affects colony formation, with a drastic reduction (65%) in the number and size of colonies, compared to vector only-transfect controls. (**b**) Confocal microscope analysis demonstrated that the MITOSTATIN-GFP colonies were indeed derived from cells not expressing MITOSTATIN, as shown by absence of green fluorescence. (**c–d**) DNA synthesis was analyzed by BrdU incorporation in Hela and 293 cell lines using two different constructs with GFP located at the N- or C-terminal ends. (**c**) Determination of BrdU incorporation showing a considerable reduction in the rate of DNA synthesis in cells transfected with MITOSTATIN, when compared with cells transfected with the vector alone in which we observed a reduction of 8.5%. Bars, 10 μm.

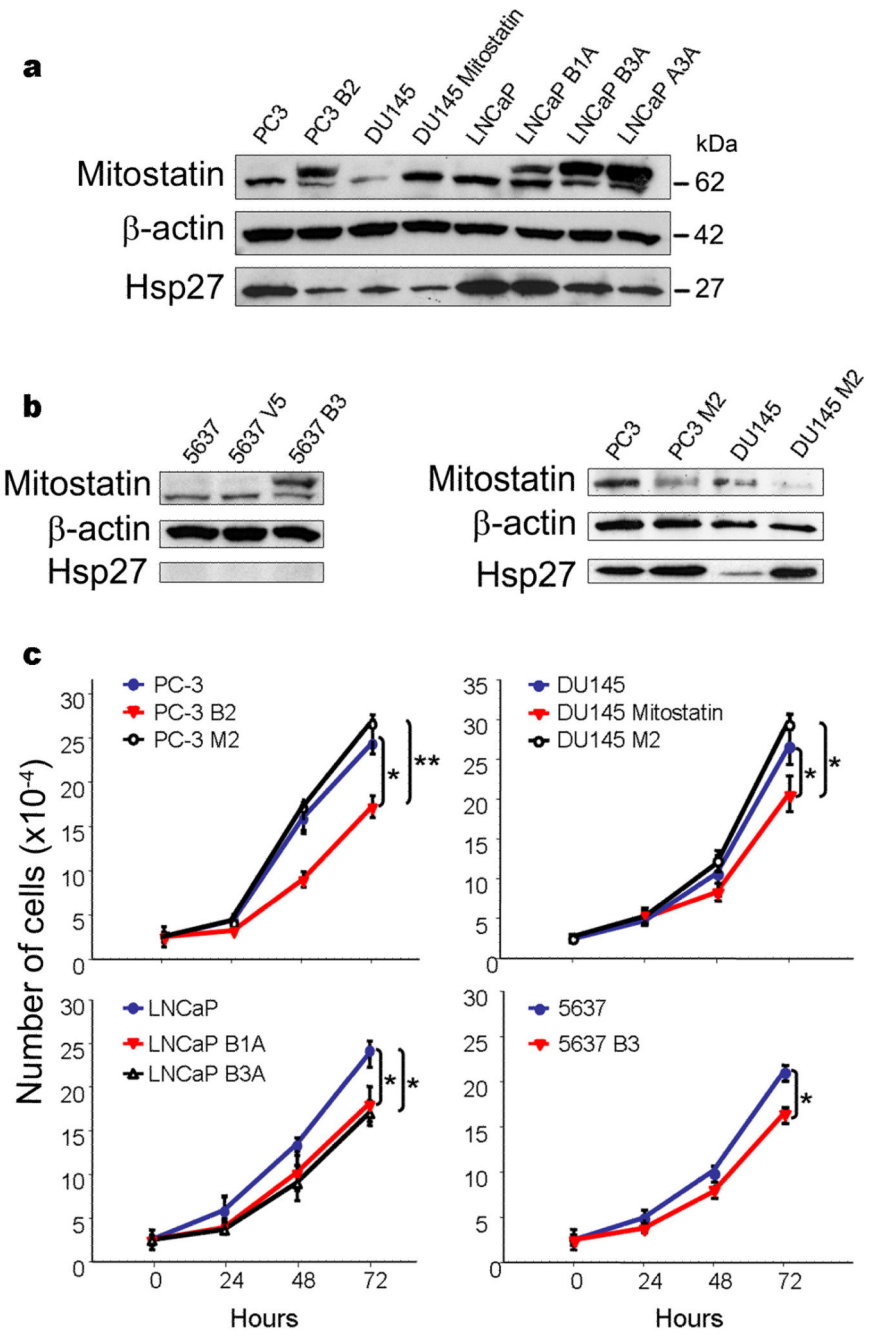

Figure 6. MITOSTATIN inhibits cell growth in bladder and prostate cancer cells by a down-regulation of Hsp27

Endogenous and ectopic MITOSTATIN protein is detected in prostate (**a**) and bladder (**b**, *left panel*) stable MITOSTATIN-transfectants cells. (**b**) A significant reduction of MITOSTATIN protein is detected in PC3 M2 and DU145 M2 cells stably transfected with a MITOSTATIN antisense-vector. Reduced Hsp27 is shown in cells over-expressing MITOSTATIN (**a**). Conversely, an increased level of Hsp27 is observed in cells with lower expression of MITOSTATIN (**b**, *right panel*). 5637 bladder cancer cells do not express

Hsp27 (**b**). (**c**) Growth curves show significant decrease in cells over-expressing MITOSTATIN when compared with parental cells and cells transfected with the MITOSTATIN-antisense plasmid. Data show the mean of three independent experiments ±SEM. * $P<0.05$ ** $P<0.01$.

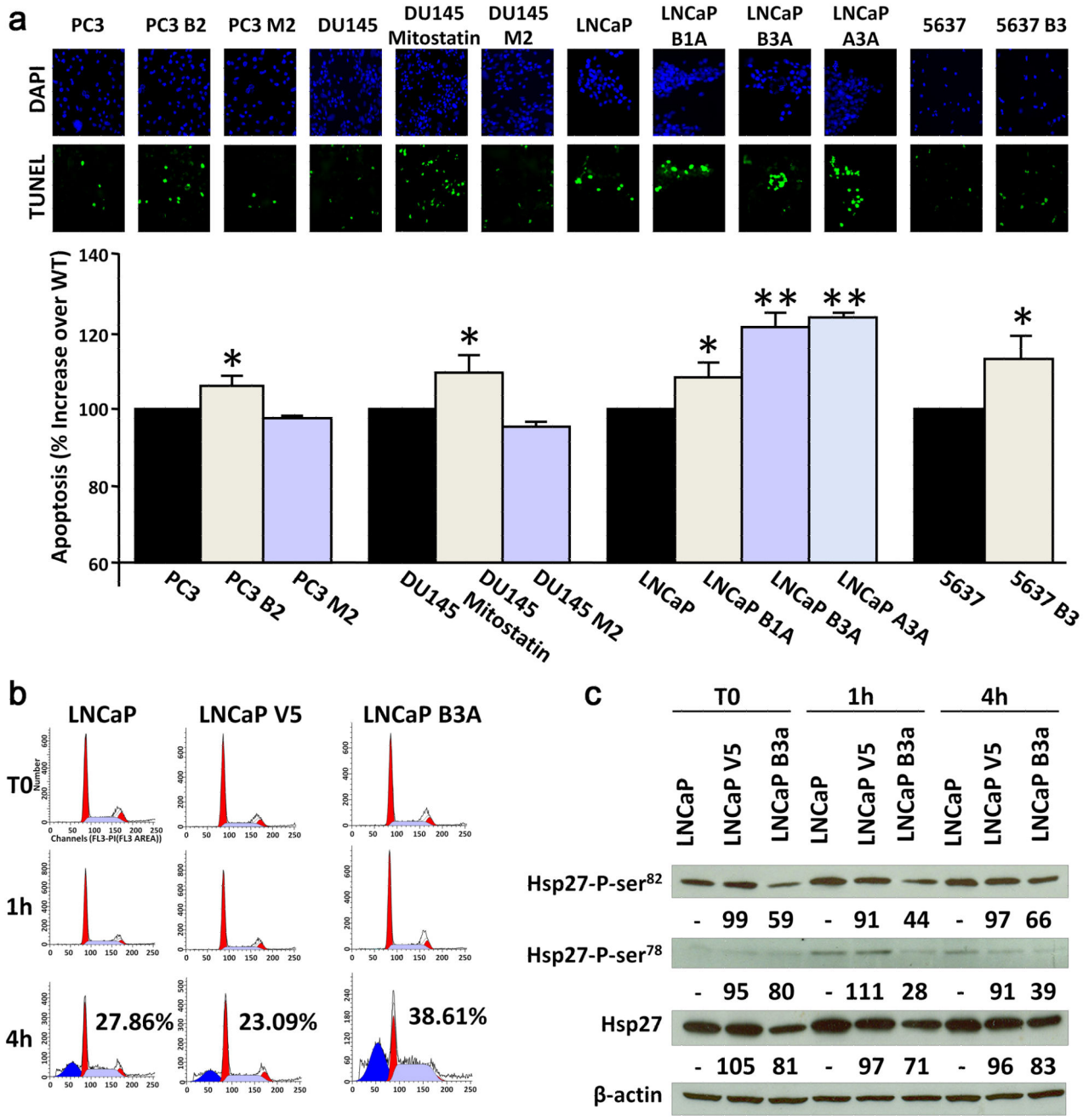

Figure 7. MITOSTATIN over-expression increases staurosporine-induced apoptosis in prostate and bladder cancer cells

(**a**) TUNEL analysis of cells after 4 h of treatment with 1μM staurosporine show a significant increase in apoptosis in cells over-expressing MITOSTATIN. *Upper panel*, representative images from three independent experiments; *bars in the lower panel*, SEM. * P<0.05 ** P<0.01. (**b**) FACS analysis of LNCaP wild type, LNCaP control vector V5 and LNCaP B3A cells after 1 h and 4 h of treatment with 1μM staurosporine. Numbers indicate the percentage of apoptotic cells in each group. (**c**) MITOSTATIN inhibits Hsp27 activation

and affects Hsp27 expression levels. Expression levels of the protein tested in comparison of the levels observed in the parental cells in three different experiments are *shown* under the blots.

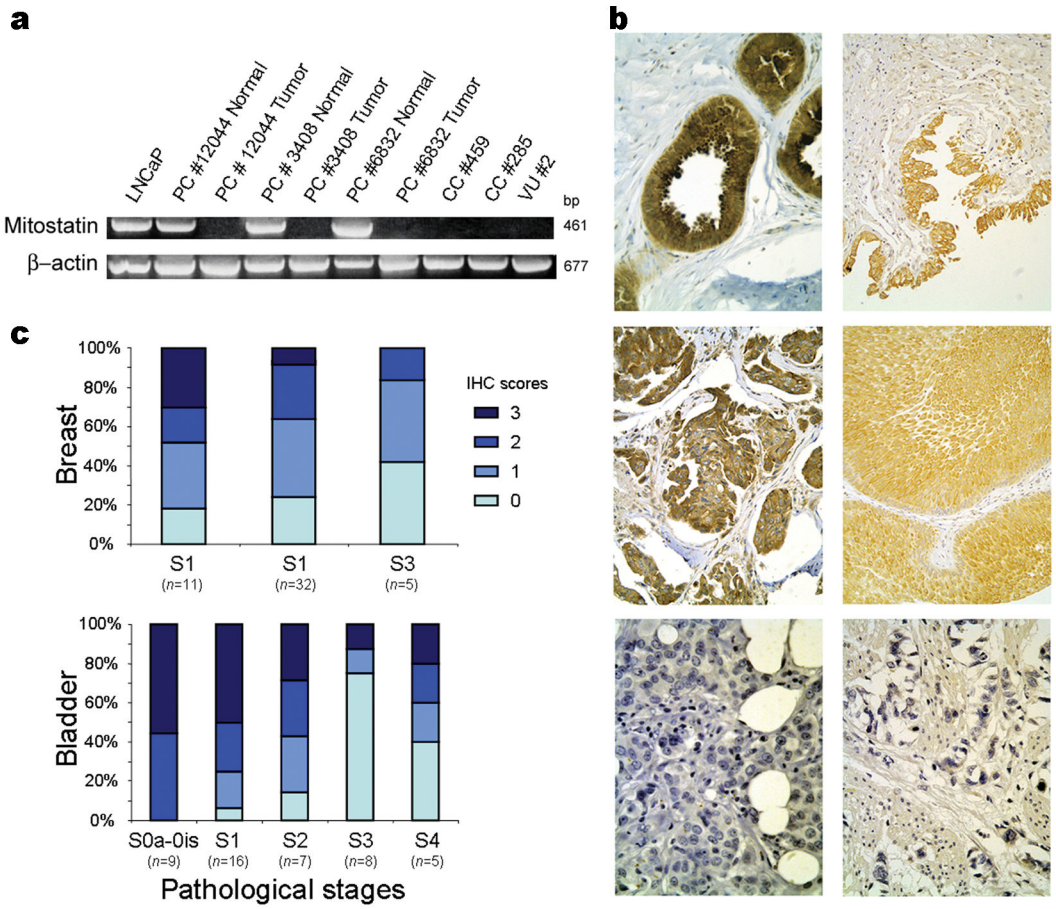

Figure 8. ***MITOSTATIN*** **is deleted in cancer, mutated in cancer cell lines and its expression is decreased in advanced tumor stages**

(**a**) *MITOSTATIN* ORF was not detected by RT-PCR in three primary prostate tumors (PC), two colon adenocarcinoma (CC) and one carcinoma of the vulva (VU). In the three prostate samples we also studied the normal counterpart in which the gene was normally expressed. (**b**) Examples of immunohistochemical detection of MITOSTATIN in human breast and bladder. MITOSTATIN cytoplasmatic staining was observed in normal breast (*upper left panel*) and bladder (*upper right panel*) human specimens. Normal mammary glands show a very intense MITOSTATIN-staining in both cytoplasm and cellular membrane (*upper left panel)*. Examples of MITOSTATIN positive breast (*middle left panel)* and bladder *(middle right panel*) cancers and negative breast (*lower left panel*) and bladder (*lower right panel*) tumors. (X400). (**c**) MITOSTATIN immunohistochemical expression is decreased in advanced stages in breast and prostate. The distribution of the immunohistochemical scores in the different tumor stages is shown. Original magnifications 10x, 20x and 40x.